ISAS - INTERNATIONAL SCHOOL FOR ADVANCED STUDIES

Ab–initio Molecular Dynamics

with

Parrinello–Rahman Deformable Cell

Thesis submitted for the degree of

"Magister Philosophiæ"

CANDIDATE

Paolo Focher

SUPERVISORS

Prof. Michele Parrinello

Dr. Guido L. Chiarotti

November 1992

TRIESTE

SISSA ISAS

SCUOLA INTERNAZIONALE SUPERIORE DI STUDI AVANZATI
INTERNATIONAL SCHOOL FOR ADVANCED STUDIES

Ab–initio Molecular Dynamics

with

Parrinello–Rahman Deformable Cell

Thesis submitted for the degree of

"Magister Philosophiæ"

CANDIDATE

Paolo Focher

SUPERVISORS

Prof. Michele Parrinello

Dr. Guido L. Chiarotti

November 1992

Acknowledgements

I would like to express my thanks to my supervisors, Michele Parrinello and Guido Chiarotti, to Erio Tosatti and Giuseppe Santoro for stimulating discussions and encouragement. I am particularly indebted to Marco Bernasconi, for his precious and continuos help.

Index

Introduction

A major issue in solid–state theory is the study of the mechanical behaviour of solids under various conditions of temperature and stress. At low temperatures traditional theories, based on the harmonic approximation, give a rather good account of the observed properties. However, a large number of systems are so much affected by anharmonicity, that the harmonic approach is bound to fail. In such circumstances Molecular Dynamics is expected to be very useful.

Crystal structure transformations are a clear example of highly anharmonic phenomenon and thus a natural candidate for Molecular Dynamics (MD) study. However, until few years ago, such studies were belived to be impossible, because of the necessity of periodic boundary conditions, used to minimize surface and finite size effects on bulk properties. The difficulty lies in the fact that structural tranformations are often associated with change in the shape of the crystal, while periodic boundary conditions prevent shape fluctuations. If one can simulate very large systems this undesired effect of boundary conditions becomes more and more irrelevant, since the system will eventually crystallize in a new phase by forming appropriate defects; it is actually crucial in dealing with small systems, to which one has often to restrict himself, even with modern computers.

Parrinello-Rahman Molecular Dynamics is a recent method, which reconciles periodic boundary conditions, essential ingredient of any MD study of bulk properties, with the possibility of changing shape and volume of the simulation cell. The usefulness of this approach has been demonstrated in the simulation of a large variety of systems using empirical expressions for the interatomic forces.

The efficancy of the method is obviously limited by the empirical nature of the potentials used in conventional MD framework. Few years ago Car and Parrinello have proposed a powerful alternative scheme for MD, where the forces are derived by using state–of–the–art electronic structure calculations, based on the Density Functional Theory. The interatomic potential is parameter–free and derived from *first principles*, with no experimental input. This method has been succesfully applied to a variety of problems which had

1

previously been inaccessible.

In this work, following the method formulated by Parrinello and Rahman for the conventional classical MD, we have extended the fixed cell *ab–initio* MD by Car and Parrinello, by including the possibility of changing shape and volume of the simulation cell.

In Section 1 we describe the original Parrinello–Rahman method, introducing some basic concepts used later on. Section 2 is devoted to the general formulation of the new *ab–initio* MD with deformable cell. In Section 3 we describe the practical calculation of the stress tensor, one of the new ingredients of the method, inside the well–known plane–wave representation of electronic wave–functions, usually adopted in Car–Parrinello simulations of solids (in the Appendix are collected the explicit formulas of the stress tensor for such a representation). Since we have finished with the practical implementation of the method and the tests of the code for computer simulations in the last few weeks, we can not yet present physically interesting results. Nevertheless in Section 4, we show two examples of minimization procedure and dynamics obtained with our code on a small cell of Silicon atoms. In the last Section we summarize the perspectives of the method.

1 Parrinello–Rahman Molecular Dynamics

In this section we will briefly review the Parrinello–Rahman[1] method (PR) for Molecular Dynamics with deformable cell. PR is the natural extension of the Andersen[2] Molecular Dynamics. In the original Andersen method the simulation cell is allowed to change its size *isotropically*, following the deviation of internal pressure from an assigned value. This is done by introducing the volume of the cell as a new dynamical variable, without renouncing to the periodic boundary conditions. In the PR method, the cell can change, more generally, both shape and size; one has, therefore, to take into account all the degrees of freedom of the cell. This is done by PR in the following way.

Let us consider a generic simulation cell for Molecular Dynamics, which can fill all the space by repeating it at infinity with periodic boundary conditions. This can be described by the three primitive Bravais vectors $(\mathbf{a}, \mathbf{b}, \mathbf{c})$. Defining the matrix

$$\mathbf{h} = (\mathbf{a}, \mathbf{b}, \mathbf{c}) \tag{1}$$

(where the vectors constitute the columns of the matrix) , the position of a generic particle in the box, in real space $(\mathbf{R})$, can be written as:

$$\mathbf{R} = \mathbf{h}\mathbf{S}. \tag{2}$$

$\mathbf{S}$ is the vector of the so called *scaled* coordinates of the particle, whose components assume values between 0 and 1 inside the cell. (In other words, in the scaled variable space, the cell is always a cube of side 1.) The relation between distances in real and in scaled coordinates will be given by the metric tensor $\mathcal{G} = \mathbf{h}^t \mathbf{h}$, so that:

$$(\mathbf{R}_i - \mathbf{R}_j)^2 = (\mathbf{S}_i - \mathbf{S}_j)^t \mathcal{G} (\mathbf{S}_i - \mathbf{S}_j). \tag{3}$$

Since we want the cell to change in time, the basic idea of Parrinello–Rahman method, in analogy with Andersen dynamics, is to consider an *extended* langrangian system, where the nine components of the matrix $\mathbf{h}$ are classical degrees of freedom, whose trajectories are determined by appropriate generalized forces. This is obtained by the original Parrinello-Rahman

3

Lagrangian:

$$\mathcal{L} = \frac{1}{2}\sum_{i=1}^{N} M_i(\dot{\mathbf{S}}_i^t \mathcal{G}\dot{\mathbf{S}}_i) - V(\mathbf{R}_1,...,\mathbf{R}_N) + \frac{1}{2}W\mathrm{Tr}(\dot{\mathbf{h}}^t\dot{\mathbf{h}}) - p\Omega, \qquad (4)$$

where M_i is the mass of i-th particle, V the classical potential, W the "mass" of the cell, p the external pressure, and, finally, $\Omega = \det \mathbf{h}$ is the volume of the cell.

One can see that the first two terms of Eq. 4 define the Lagrangian for the usual fixed cell Molecular Dynamics. Note also that when the cell varies in time the kinetic term in Eq. 4 does not correspond to the actual kinetic energy of the particles in the real system.

The Euler-Lagrange equations of motion derived from Eq. 4 are:

$$\ddot{\mathbf{S}}_i^\alpha = -\frac{1}{M_i}\frac{\partial V}{\partial \mathbf{R}_i^\beta}\mathbf{h}_{\beta\alpha}^{t-1} - \mathcal{G}_{\alpha\beta}^{-1}\dot{\mathcal{G}}_{\beta\gamma}\dot{\mathbf{S}}_i^\gamma, \qquad (5)$$

$$\ddot{\mathbf{h}}_{\alpha\beta} = \frac{1}{W}(\Pi_{\alpha\gamma} - p\delta_{\alpha\gamma})\Omega\mathbf{h}_{\gamma\beta}^{t-1}, \qquad (6)$$

where:

$$\Pi_{\alpha\gamma} = \frac{1}{\Omega}\left(\sum_i M_i\mathbf{v}_i^\alpha\mathbf{v}_i^\gamma - \frac{\partial V}{\partial \mathbf{h}_{\alpha\delta}}\mathbf{h}_{\delta\gamma}^t\right), \qquad (7)$$

and

$$\mathbf{v}_i^\alpha = \mathbf{h}_{\alpha\gamma}\dot{\mathbf{S}}_i^\gamma. \qquad (8)$$

(We will always use greek indices to indicate the components of vectors and matrices. The convention of implicit sum over repeated indices is assumed.)

Notice that, interpreting $M_i\mathbf{v}_i$ as the momentum of i-th particle, Π is nothing but the internal stress tensor. This can be seen by comparing the second term of Π with the usual definition of internal stress tensor coming from the theory of elasticity:[3]

$$\pi_{\alpha\beta} = -\frac{1}{\Omega}\frac{\partial V}{\partial \epsilon_{\alpha\beta}}, \qquad (9)$$

where ϵ is the strain tensor with respect to the present configuration. Let in fact ϵ be a small strain of the system, which deforms the cell from $\mathbf{h}$ to

$h' = h + dh$; we have:

$$R = hS$$
$$R' = (1 + \epsilon)R = h'S$$
$$= h'h^{-1}R.$$

Therefore, to first order in dh:

$$\epsilon = h'h^{-1} - 1, \tag{10}$$

from which we obtain:

$$\frac{\partial V}{\partial h}h^t = \frac{\partial V}{\partial \epsilon}. \tag{11}$$

From Eq. 6 we see that the "forces" on the cell are therefore proportional to the difference $(\Pi - p)$, which implies that the time variation of matrix h is driven by the imbalance between external pressure and total stress.

The Lagrangian (Eq. 4) is conservative; and therefore admits a constant of motion, given by:

$$\mathcal{H} = \frac{1}{2}\sum_i M_i v_i^2 + V(R_1, ..., R_N) + p\Omega + \frac{1}{2}W\mathrm{Tr}(\dot{h}^t\dot{h}). \tag{12}$$

Physically $\langle \mathcal{H} \rangle$ corresponds to the enthalpy of the system,[4] apart for the last term, which becomes negligible for large N (its contribution to $\langle \mathcal{H} \rangle$ at equilibrium is $\frac{9}{2}k_BT$).

It has been shown[5,2] that trajectories generated with PR dynamics give averages of thermodynamical quantities that are in fact equivalent in the thermodynamical limit to the Gibbs averages in the (H,p,N) statistical ensemble, i.e. the ensemble with enthalpy, pressure and number of particles kept constant.

To conclude this introduction to the PR formulation we briefly point out some considerations on the role played by the parameter W. In the equations this quantity is the "mass" of the cell, in the sense that it is related to the *inertia* of h. It is clear that W does not influence equilibrium properties, since in classical mechanics the equilibrium properties of a system do not depend on the mass of the constituents. This is however no longer true for dynamical properties. Andersen has suggested a physical criterion for the

5

choice of W: W should be tuned so as to obtain a relaxation time of the cell of the order of $\tau = L/c$, where L is the linear dimension of the cell and c the sound velocity inside the system. From a slightly different point of view, one can estimate the characteristic frequency of the cell by linearizing Eq. 6. Assuming this frequency to be roughly $1/\tau$, one obtains:[4] $W = 3\sum_i M_i/4\pi^2$.

2   Extension to Ab-initio Molecular Dynamics

We want now to extend the previous formulation of the original Parrinello–Rahman method to the case of Car–Parrinello *ab–initio* Molecular Dynamics (CP).[6,7]

In this recent and powerful method, the forces acting on classical ionic degrees of freedom are calculated not from a parameter–dependent potential – usually determined via an empirical *ad hoc* procedure – but from a quantum treatement of the electronic system based on Density Functional Theory (DFT)[8-10] in a consistent way as the simulation proceeds. This is done by introducing a fictitious dynamics for the electronic wave–functions (treated as classical scalar fields) that allows the electrons to follow adiabatically the ionic motion, remaining close to their Born–Oppenheimer surface.

The problem of extending this method to the case of a deformable cell is in principle the same as for classical systems. One would like to take into account shape and volume changes of the simulation cell by considering the extended system obtained by rewriting the original Lagrangian in scaled coordinates with the two additional terms pertaining to the cell (last two terms of Eq. 4).

The presence of the electonic wave–functions in the CP Lagrangian[7] makes this procedure slightly more subtle. We want indeed to write a new classical Lagrangian, which reduces to the original CP Lagrangian in the fixed cell case, and in which the degrees of freedom are some scalar fields ψ (not explicitely dependent on h) associated to the electrons, the scaled ionic coordinates S and the cell matrix h. We also want to preserve the physical meaning of PR equations of motion. It is clear that the original wave–functions $\psi_h(\mathbf{r})$ (where the lower index h indicates a wave–function defined and normalized on the cell generated by h) are no longer a good candidate for being the scalar field of our Lagrangian, because of the dependence on the cell. We have to decide how to scale them. The natural way to do this, which has several advantages, as we shall see in the following, is to define a wave–function $\psi(\mathbf{s})$ onto the scaled variable space $\mathbf{s} = \mathbf{h}^{-1}\mathbf{r}$ (normalized on

the unitary cube), such as:

$$\psi_h(\mathbf{r}) = \frac{1}{\sqrt{\Omega}}\psi(\mathbf{h}^{-1}\mathbf{r}) = \frac{1}{\sqrt{\Omega}}\psi(\mathbf{s}), \qquad (13)$$

where the prefactor $1/\sqrt{\Omega}$ preserves the normalization. $\psi(\mathbf{s})$ is really independent on $\mathbf{h}$. From Eq. 13 follows the transformation law for the electronic charge density, which appear in the DFT energy functional (see Eq. 20 in the next section):

$$\rho_h(\mathbf{r}) = \frac{1}{\Omega}\rho(\mathbf{h}^{-1}\mathbf{r}). \qquad (14)$$

This choice for the tranformation of the wave–functions corresponds to consider that the only *direct* effect of the deformation of the cell on the wave–functions and on the electronic density in real space is a "stretching" of them, in order to satisfy the changed boundary conditions.

Let us write now the new Lagrangian as:

$$\mathcal{L} = \mu\sum_i \int ds\, |\dot{\psi}_i(\mathbf{s})|^2 + \frac{1}{2}\sum_I M_I(\dot{\mathbf{S}}_I^t \mathcal{G}\dot{\mathbf{S}}_I) - E\left[\{\psi_i\}, \{\mathbf{h}\mathbf{S}_I\}\right] +$$

$$\sum_{ij}\Lambda_{ij}\left(\int ds\, \psi_i^*(\mathbf{s})\psi_j(\mathbf{s}) - \delta_{ij}\right) + \frac{1}{2}W\mathrm{Tr}(\dot{\mathbf{h}}^t\dot{\mathbf{h}}) - p\Omega, \qquad (15)$$

where the integrals are taken on the scaled cell. μ is the fictitious mass of the electrons, E is the DFT total energy functional and Λ_{ij} are the Lagrangian multipliers associated with the orthonormalization constraints of the wave–functions. The sums over i and j are taken on the electronic states, and the sum over I on the ions. Notice that if the cell is kept fixed, Eq. 15 reduces to the original CP Lagrangian, written for the scaled wave–functions, apart for the constant term $p\Omega$. In fact, using the Eq. 13 and changing the integration variable, one obtains immediately that the integrals in the first and fourth term of Eq. 15 are invariant under scale transformation; for instance:

$$\int \psi^*(\mathbf{s})\psi(\mathbf{s})d\mathbf{s} = \Omega\int \psi_h^*(\mathbf{h}\mathbf{s})\psi_h(\mathbf{h}\mathbf{s})d\mathbf{s} = \int \psi_h^*(\mathbf{r})\psi_h(\mathbf{r})d\mathbf{r}. \qquad (16)$$

Notice also that using the scaled wave–functions, we neglect in the kinetic term (first term of Eq. 15) the contribution due to the deformation of the cell (exactly in the same way as in Eq. 4 this contribution to the kinetic energy

8

of the ions is neglected) This ensures that the CP equations of motion for the electronic wave–functions are not modified by the new Lagrangian.

The equations for ionic degrees of freedom have exactly the same form as in classical PR case (see Eq. 5), with the replacement of the classical forces $-\partial V/\partial \mathbf{R}$ by $-\partial E/\partial \mathbf{R}$. Thanks to the Hellmann–Feynmann theorem, these classical partial derivatives give the actual quantum–mechanical forces acting on the ions.[11]

The independence of the integrals in Eq. 15 on h ensures also that no extra terms with respect to Eq. 6 appear in the equations for the cell parameters. Here in the tensor Π (Eq. 7) $\partial V/\partial \mathbf{h}$ is replaced by $\partial E/\partial \mathbf{h}$. This is the partial derivative of a functional of classical fields and coordinates, and one would like to show that it is nothing but the quantum–mechanical internal stress tensor. Only in this case the extension of PR Dynamics in the *ab–initio* scheme would be complete and physically interesting.

If we consider the electronic quantum Hamiltonian of our system and the ground state Ψ_o for a generic configuration of the cell (h) and the ions, then $E = \langle \Psi_o | H | \Psi_o \rangle$ (apart the small deviations due to the oscillations of wave–functions around their instantaneus ground–state in the CP dynamics). In close analogy to the Hellmann–Feynmann theorem, it can be shown[12,13] that to calculate $\partial E/\partial \mathbf{h}$ at a generic h it is not necessary to know how does the ground–state modify under the perturbation ($d\mathbf{h}$), since from the variational property of E a perturbation of the ground–state does not change E to first order. We can therefore calculate the derivative of E as the expectation value on Ψ_o of the derivative of the electronic Hamiltonian, *i.e.* the partial derivative inside E, keeping the wave–functions constant. However one has to pay attention in the present case to the "stretching" of the unperturbed ground–state wave–functions: since the wave–functions satisfy boundary conditions, which are changed by the perturbation, it is necessary to rescale the "streched" functions such as to preserve their normalization on the perturbed cell. This is automatically taken into account by replacing $\psi_h(\mathbf{r})$ with $\psi(\mathbf{s})$ using Eq. 13. This indeed implies that the term $(\partial E/\partial \mathbf{h})\mathbf{h}^t$ (see also Eq. 11) appearing in Π (Eq. 7) is the actual quantum–mechanical stress tensor, as we want.

9

Summarizing, we have shown in this section how it is possible to extend in a general and natural way the PR method into the CP Molecular Dynamics. All the equations of motion derived from the Lagrangian in Eq. 15 can be formally written as:

$$\mu\ddot{\psi}_i(\mathbf{s}) = -\frac{\delta E}{\delta\psi_i^*(\mathbf{s})} + \sum_j \Lambda_{ij}\psi_j(\mathbf{s}) \tag{17}$$

$$\ddot{S}_i^\alpha = -\frac{1}{M_i}\frac{\partial E}{\partial R_i^\beta}h_{\beta\alpha}^{t-1} - \mathcal{G}_{\alpha\beta}^{-1}\dot{\mathcal{G}}_{\beta\gamma}\dot{S}_i^\gamma, \tag{18}$$

$$\ddot{h}_{\alpha\beta} = \frac{1}{W}\left(\Pi_{\alpha\gamma} - p\delta_{\alpha\gamma}\right)\Omega h_{\gamma\beta}^{t-1}. \tag{19}$$

In the next section we describe the explicit derivation in the framework of CP method of the internal stress tensor, the only quantity which is still lacking for a practical implementation of the *ab–initio* Molecular Dynamics with deformable cell.

3 Stress Tensor from DFT–LDA Total Energy

Consider a system of N atoms and M electronic states ($\{\psi(\mathbf{r})\}$) in a cell generated by h. (For semplicity we consider in the following just one atomic species, the extension to more than one species being trivial.) The interaction between electrons and ions is described by using ab–initio pseudopotentials.[14,15] For such a system, the DFT total energy E in Local Density Approximation (LDA)[16,17] can be written as:

$$E\left[\{\psi_i\}, \{\vec{R}_I\}\right] = \sum_i^{occ} f_i \int d\vec{r}\, \psi_i^{\times}(\vec{r}) \left(-\frac{1}{2}\nabla^2\right) \psi_i(\vec{r}) + \int d\vec{r}\, V^{ext}(\vec{r}) \rho_e(\vec{r})$$

$$+ \frac{1}{2} \int d\vec{r} d\vec{r}\,' \frac{\rho_e(\vec{r})\rho_e(\vec{r}\,')}{|\vec{r} - \vec{r}\,'|} + E_{xc}\left[\rho_e\right] + \sum_{I \neq J} \frac{Z_v^2}{\left|\vec{R}_I - \vec{R}_J\right|}. \quad (20)$$

V^{ext} is the total ionic potential, expressed as a sum of ionic pesudopotentials v_{ps}; $\rho_e(\vec{r}) = \sum_i^{occ} f_i |\psi_i(\vec{r})|^2$ is the electronic charge density, f_i the occupation numbers of electronic states, Z_v is the valence charge density of the atoms, and E_{xc} the exchange–correlation energy functional, which is expressed within LDA.

The simulation cell is periodically repeated to infinity and, as a consequence of the periodicity, the electronic wave–functions can be expanded in plane–waves.[18] Since we sample only the Γ–point of the Brillouin zone, a generic wave–function can be written as:

$$\psi_h(\mathbf{r}) = \frac{1}{\sqrt{\Omega}} \sum_{\mathbf{G}} c_h(\mathbf{G}) e^{i\mathbf{G}\cdot\mathbf{r}}. \quad (21)$$

The basis set for the expansion in Eq. 21 is reduced to a finite set by truncating the sum over $\mathbf{G}$ to include only those plane–waves with a kinetic energy $K = \frac{1}{2}\mathbf{G}^2$ less than a given energy E_{cut}. (Atomic units are used in the following.) It is clear that the choice of E_{cut} determines the accuracy of the calculation of the DFT energy, and its value depends on the specific system.

Since we use plane–waves, it is much more convenient to evaluate all terms of Eq. 20, except E_{xc}, in the Fourier space.[11] In order to calculate $\partial E/\partial$h as described in previous section, we have to be able to isolate the dependence

of E on $\mathbf{h}$ also in Fourier space. It is therefore useful to introduce the *scaled* reciprocal vectors, *i.e.* the reciprocal vectors of unitary cube:

$$\mathbf{q} = 2\pi \begin{pmatrix} h \\ k \\ l \end{pmatrix}, \qquad h, k, l \text{ integers.} \tag{22}$$

Consider now the reciprocal vector in *real* variables:

$$\mathbf{G} = h\mathbf{b}_1 + k\mathbf{b}_2 + l\mathbf{b}_3. \tag{23}$$

From the definition of primitive reciprocal vectors $\mathbf{b}_i$ and the definition of $\mathbf{h}$ (Eq. 1), one gets:

$$\mathbf{G} = \mathbf{h}^{t-1}\mathbf{q}, \tag{24}$$

which is the transformation law of coordinates in reciprocal space. Using Eqs. 2, 13 and 24 it is easy to get the transformation for wave–functions in Fourier space:

$$c_h(\mathbf{G}) = \frac{1}{\Omega} \int d\mathbf{r}\, e^{-i\mathbf{G}\cdot\mathbf{r}} \psi_h(\mathbf{r}) = \int d\mathbf{s}\, e^{-i\mathbf{q}\cdot\mathbf{s}} \psi(\mathbf{s}) = c(\mathbf{q}). \tag{25}$$

This equation states that the $c_h(\mathbf{G})$ are invariant under scale tranformation. They are in fact the electronic degrees of freedom in Fourier space, whoose equations of motion from Eq. 17 are therefore the same in real or in scaled variables.

We have now all the basic ingredients to evaluate the expicit formulas for the stress tensor $\partial E/\partial \mathbf{h}$. The calculations are straightforward but boring in some cases and we address the reader to the Appendix for the results.

Concluding this section we will point out some considerations about the well known problems arising from using a finite basis set of plane–waves in the expansion of Eq. 21. Plane–waves are very appealing, because they are independent of the structure of the system, and systematic improuvements of the quality of the basis set can be simply done by increasing the number of Fourier components. Furthermore, fast Fourier transform techniques can be adopted in the practical calculation of E. The difficulty encountered when using plane–waves is mainly ralated to the problem of convergence in Fourier

space, i.e. to the question: how small cut–off energy E_{cut} will suffice in order to shrink the errors due to a finite Fourier series to negligible values?

In the present case we are interested in performing calculations of DFT functional E, while the simulation cell varies in shape and volume. This implies that also the reciprocal space varies and, consequently, the set of plane–waves with kinetic energy less than E_{cut} does the same. In the CP method, however, the number of plane–waves (N_{pw}) is kept constant to its initial value. This implies that wave–functions, charge densities and potentials appearing in the functional E are resolved with variable precision. Let us imagine for semplicity an isotropic volume change of the cell. If the volume decreases and N_{pw} remaines constant, the effective energy cut–off will become higher and higher and the corresponding curve E versus volume will be distorted with respect to an analogus curve calculated with constant E_{cut}. These discrepances gives, for instance, different static quilibrium properties. Although in principle both this curves are wrong and only at convergence in Fourier space they will coincide with the right one, the most common experience[19,20] shows that when choosing a constant E_{cut} the incomplete convergence leads to smaller errors in the static equilibrium. This can be explained better by an example: Fig. 1 (taken from Ref. [19]) shows the total energy of GaAs as a function of lattice constant. It can be seen that neither of the two upper curves are fully converged, but the one corresponding to constant energy cut–off is actually closer to the exact result.

A modification of the Lagrangian in Eq. 15 for a finite plane–wave basis set, is coincevable in order to perform a constant cut–off simulation. For instance, we can start with a large number of plane–waves, corresponding to the presumed maximum volume during the modification of the cell, and weigh the Fourier coefficients $c(G)$ of wave–functions by an appropriate prefactor $f(G - G_{cut})$, which smoothly switches off the contribution of those plane waves, whose wave vector becomes larger than the cut–off. However in this framework an expression of the stress tensor as the derivative of total energy at constant cut–off is needed. Since the stress calculated in the Appendix corresponds in any case to a *locally constant* number of waves, it has to be corrected by the so called Pulay stress. Several expressions for the Pulay

stress have been proposed in the literature;[21] their efficiency in *ab–initio* simulations at constant cut–off must be checked.
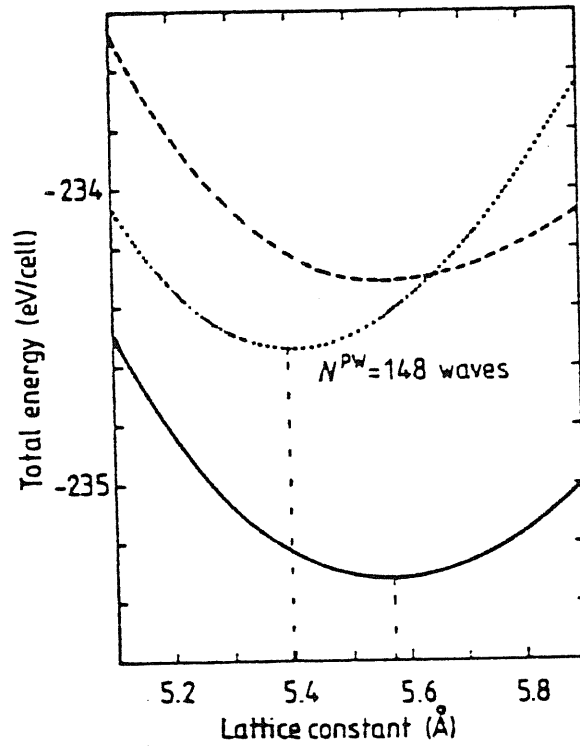

Figure 1: Total energy of GaAs as a function of lattice constant. (From Ref. [19].) The broken curve corresponds to a constant energy cut–off $E_{cut} = 12$ Ryd. Dotted curve to a fixed number of plane waves, equivalent to 12 Ryd at a lattice constant $a = 5.65$ Å(the intersection of the two curves). The solid curve corresponds to a fully converged calculation ($E_{cut} = 24$ Ryd at $a = 5.65$ Å).

4 Tests and Simple Examples of Dynamics

In this section we will present the first simple tests made with the CP code modified by the implementation of the stress tensor calculation (Eqs. in the Appendix) and by the equations of motion (Eqs. 17, 18, 19).

We test the code on a small and not computationally demanding system: a cell with 8 Silicon atoms in the diamond phase, using the Bachelet–Hamann–Schlüter pseudopotential[15] in the separable form of Kleinman and Bylander.[22] Since we sample only the Γ–point of the corresponding Brillouin zone, the results of the tests are not expected to be in good agreement with experimental data. We choose to compare them with usual total energy DFT-LDA calculations with the same cell.

Since we work at constant plane–wave number (see previous section), we decided to fix the basis set corresponding to a cut–off $E_{cut} = 18$ Ryd for the cubic cell with lattice parameter $a = 10.6$ a.u. With this basis, we have computed the ground–state energy for the cubic cell with different lattice parameters, and the 8 atoms in the perfect crystal sites. We then fitted this points with the Murnaghan equation of state, obtaining the solid curve in Fig. 2. This curve has the minimum at $E_{min} = -31.3897$ a.u. for $a = 10.428$ a.u. In Fig. 2 is also plotted the curve $E(a)$ at constant E_{cut} (dotted line). This curve gives an equilibrium lattice parameter $a = 10.469$ a.u. and $E_{min} = -31.3872$.

4.1 Optimal Lattice Structure of Silicon

As first test we made an optimization of the cell parameters. The starting cell is a FC triclinic cell with sides $a = 10.62$ a.u., $b = 10.70$ a.u., $c = 10.32$ a.u., and angles between them of 92, 96 and 88 degrees. Scaled coordinates of the atoms are near the perfect crystal positions (only a small randomization is done). The starting configuration of electronic wave–functions is the ground–state corresponding to such a cell. The optimization is performed by a combined steepest–descent for the degrees of freedom of the Lagrangian in Eq. 15. The external pressure is set to zero. The geometry of the cell and the energy E at the end of the minimization is thus expected to correspond
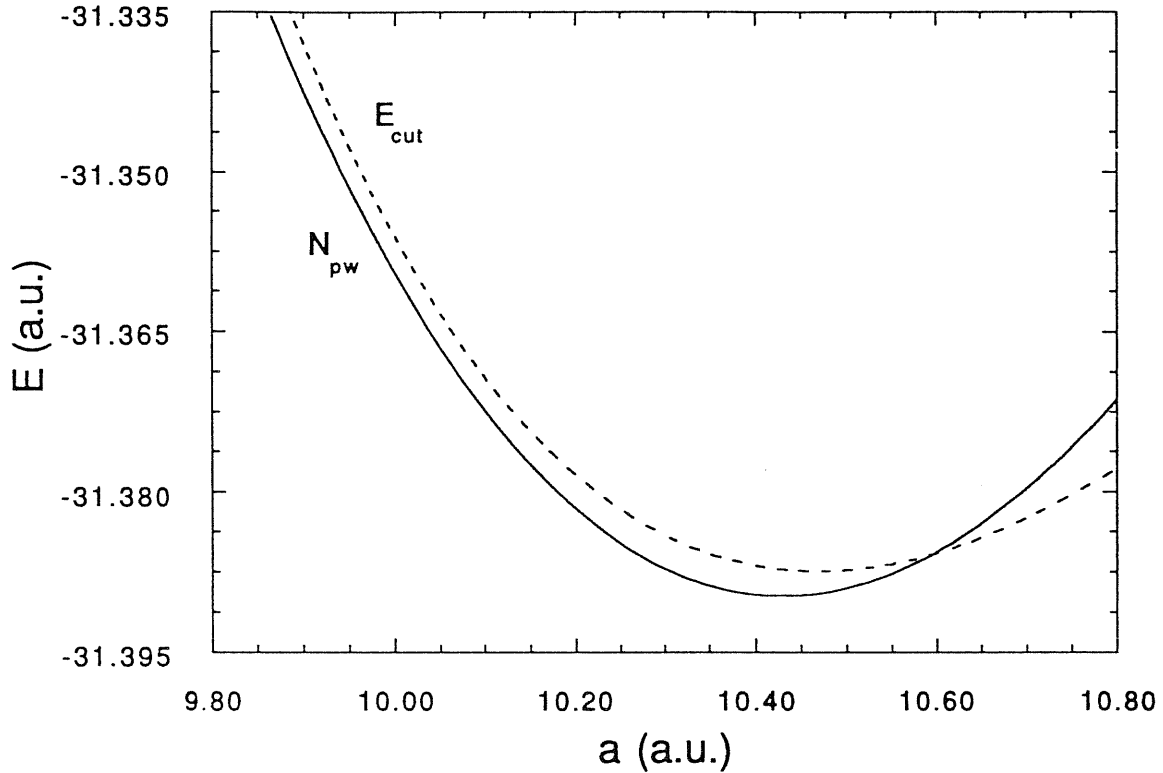
Figure 2: DFT-LDA total energy for a conventional FCC cell for diamond-silicon versus lattice parameter. The solid line corresponds to a calculation with constant number of plane waves, corresponding to a cut-off $E_{cut} = 18$ Ryd at $a = 10.7$ a.u.; dotted line corresponds to constant cut-off $E_{cut} = 18$ Ryd. Both curves are obtained by fitting some points with Murnaghan equation of state.

to the minimum of the solid curve in Fig. 2. The results are shown in Fig. 3 and 4. It can be seen the good performance of the minimization: final values for the energy and for the cell parameters are in excellent agreement with the predictions of Fig. 2. One can see that the energy E converges very rapidly to its final value (constant up to one part over 10^{-7} after 200 steps of minimization). The convergence of the stress tensor (in Fig. 4 we plotted
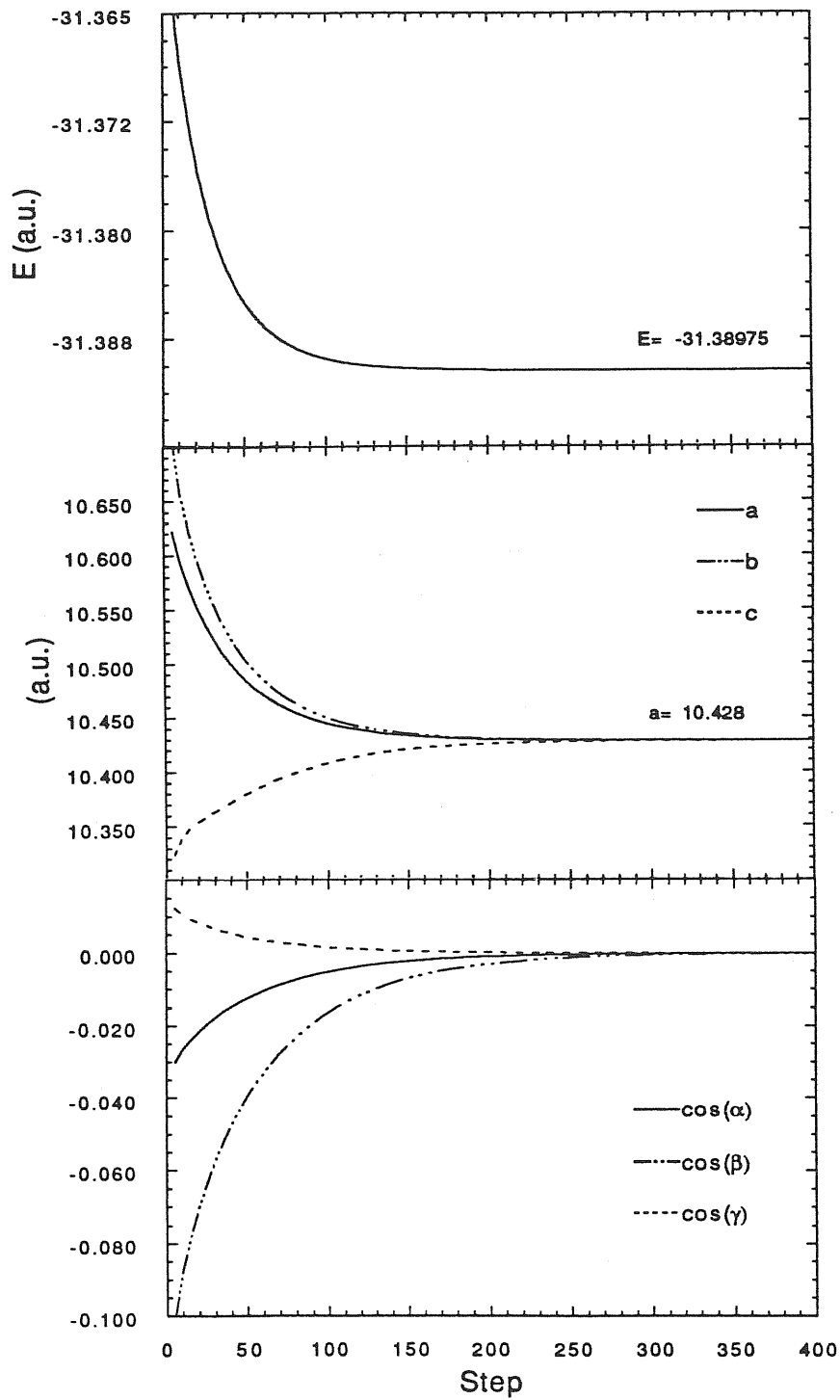
Figure 3: Results of the Steepest Descent optimization described in the text. From the upper panel to the lower there is plotted the DFT energy (E), the three sides of the cell (a, b and c), and the cosine of the angles betwen them (α is the angle between a and b, β the one between a and c and γ the one between b and c).
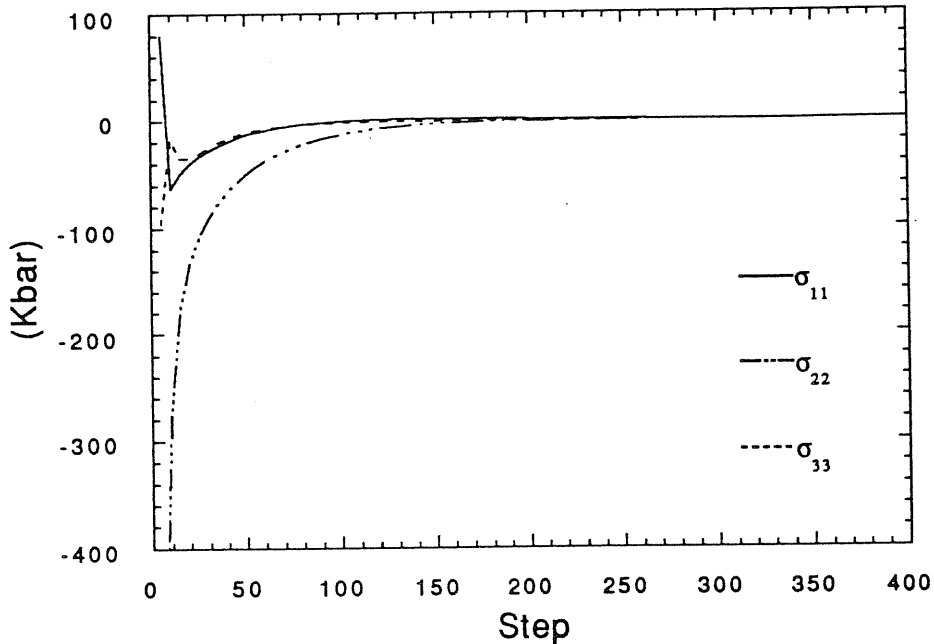
17

Figure 4: Diagonal components of the internal stress tensor during the Steepest Descent described in the text. The convergence is up to 10^{-2} Kbar after 400 minimization steps.

the behaviour of the diagonal components of the stress) and of the cell parameters is slightly slower and other 200 steps are needed in order to obtain vanishing stress up to 10^{-2} Kbar. This different rate of convergence is due to the variational nature of the energy, but not of the stress, which is therefore a better quantity for monitoring the convergence.[19]

4.2 Dynamics with Variable Cell

We will present here a simple example of free dynamics at constant pressure. The simulation cell is very small (the same cell used for the previous minimization). This implies both a bad description of the electronic structure of the system, by using the only Γ point in the Brillouin zone, and too few degrees of freedom for a resonable Molecular Dynamics calculation of correla-

tion functions. The simulation we made has therefore no physical relevance. We are in fact interested in checking the algorithm of discrete integration of Eqs. 17, 18 and 19. The starting configuration is obtained by deforming the previous optimized cell: the sides of the cell are varied by about 5% of the equilibrium value, and the angles in a range of 6 degrees around the right angle. The ionic *scaled* coordinates deviates from the perfect crystal sites by a small randomization. The "mass" W of the cell is kept as small as to ensure cell fluctuations detectable in the short physical time of the simulation. Thus, we expect to observe oscillations of the volume and of the shape of the cell roughly around the equilibrium configuration. We can also verify, in so doing, the relative mechanical stability of the optimized structure under cell fluctuations.

The simulation proceeds for 1000 steps (1 step is 5 a.u.), which correspond to a very short time: 0.12 ps. The results are shown in Figs. 5, 6 and 7. The constant of motion (Eq. 12) is conserved very well during the simulation. All the parameters of the cell (Fig. 6) oscillate with non apparent drift, but the mean values of this parameters, obtained by averaging over the whole time interval, slightly differ from the equilibrium values, due to the anharmonicity of the system. For instance, for the cell sides we obtained:

$$\langle a \rangle = 10.452 \pm 0.005 \text{a.u.}$$
$$\langle b \rangle = 10.47 \pm 0.01 \text{a.u.}$$
$$\langle c \rangle = 10.465 \pm 0.002 \text{a.u.},$$

which have to be compared to the equilibrium lattice parameter of 10.428 a.u. In Fig. 7 are shown the fluctuations of ionic temperature (solid line), calculated from the first term of Eq. 12 and the kinetic energy associated to the cell (dotted line), *i.e.* the last term of Eq. 12.
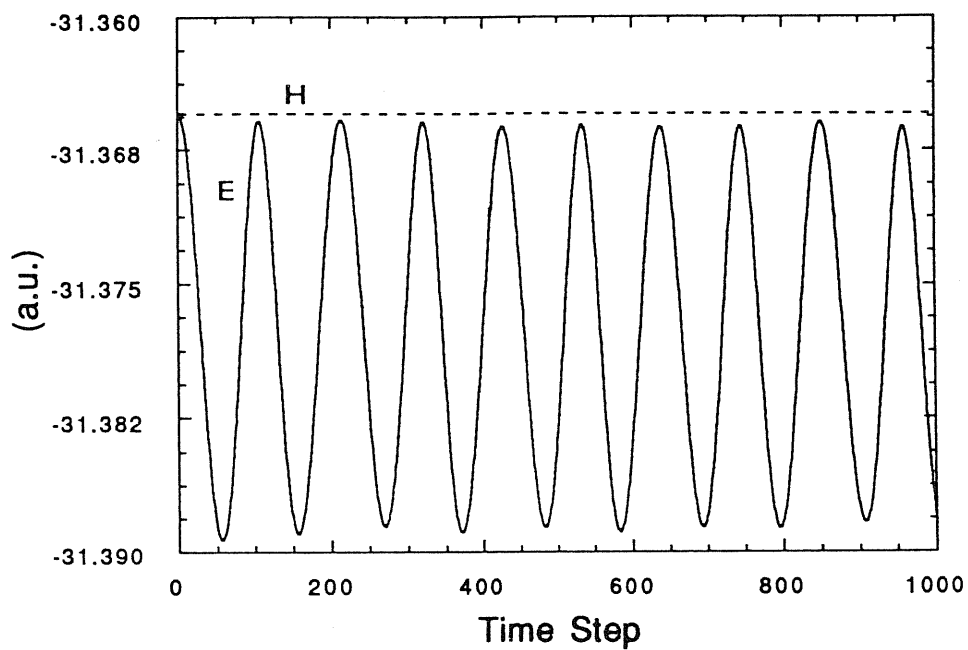
19

Figure 5: Free dynamics simulation: the cell is allowed to move. Here are plotted the constant of motion H (dotted line) and the energy E as a function of time (1000 integration steps are 0.12 ps) for the example described in the text.
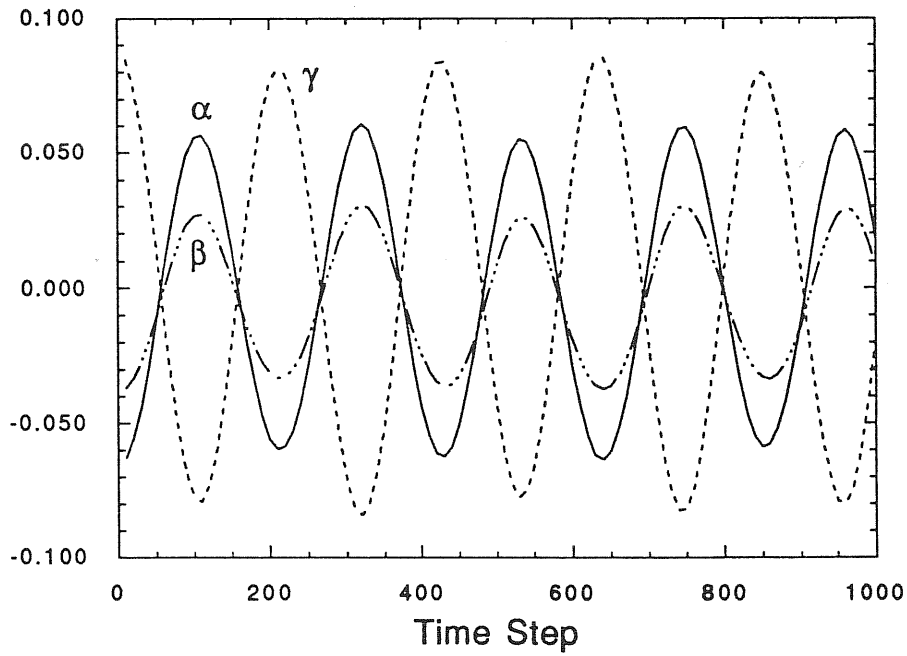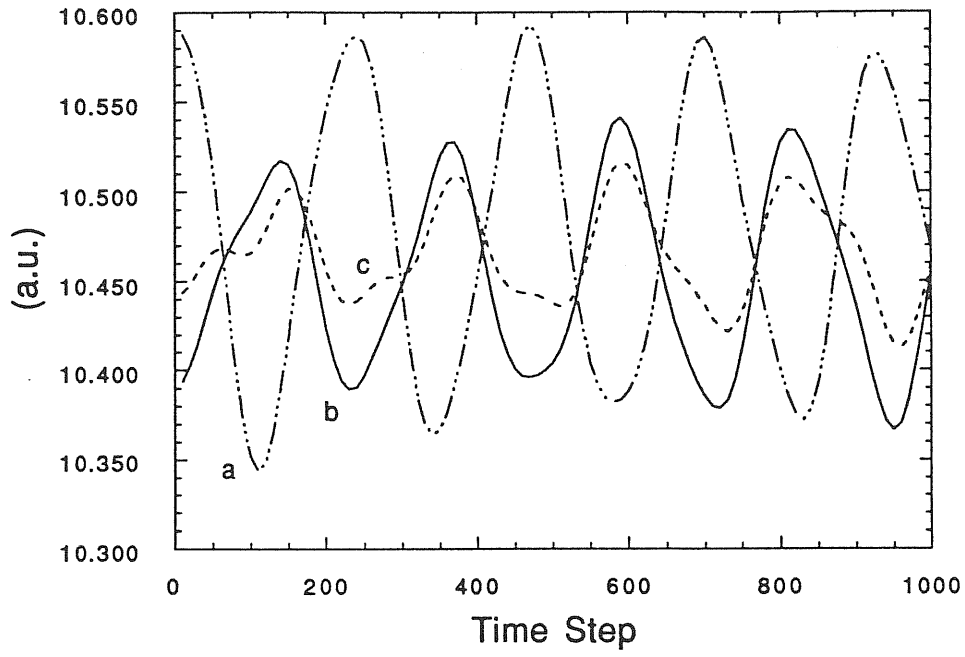
Figure 6: Cell parameters as a function of time for the free–cell dynamics simulation. In the upper panel are plotted cell sides a (broken line), b (solid) and c (dotted). In the lower panel are shown the cosines of the angles between a and b (solid line), between a and c (broken line) and between b and c (dotted).
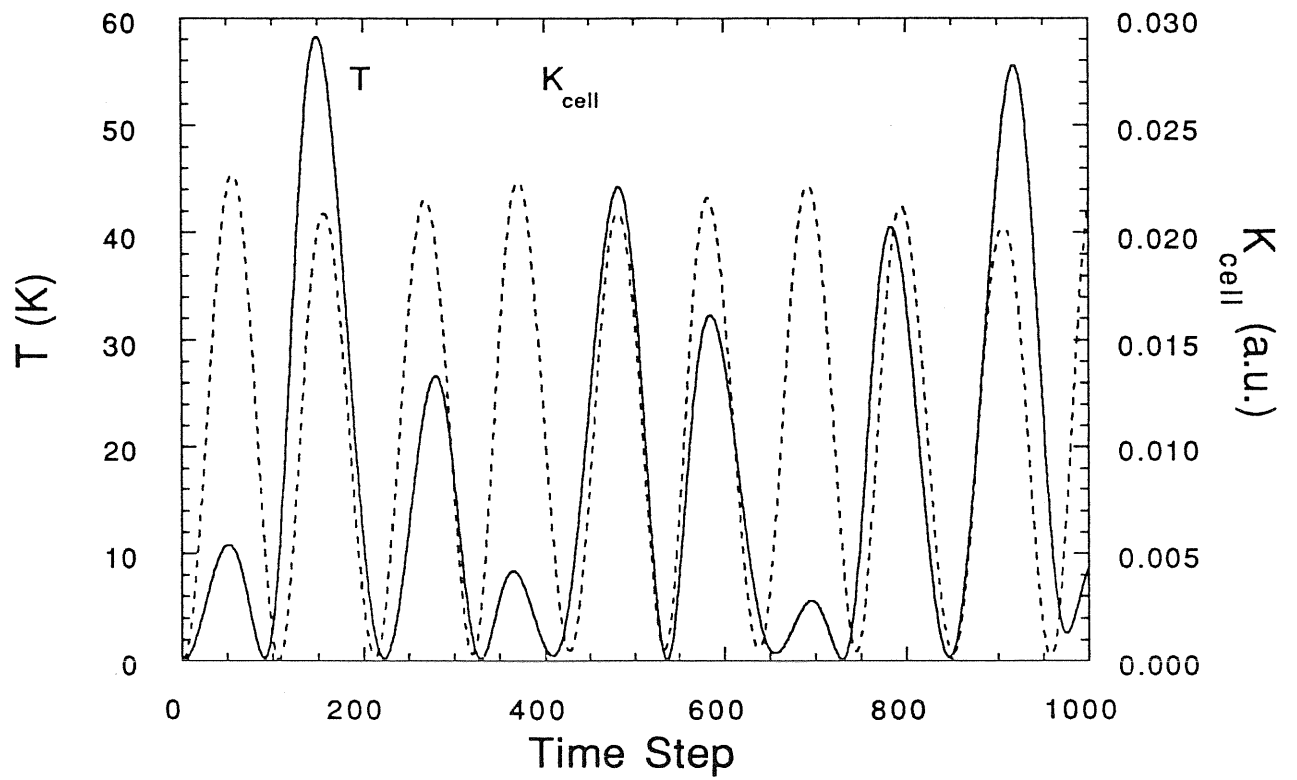
21

Figure 7: Ionic temperature and cell kinetic energy as a function of time for the free-cell dynamics simulation.

5   Future Applications and Perspectives

The CP–PR *ab–initio* Molecular Dynamics with deformable cell, presented in the previous sections, opens the possibiliy of new *ab–initio* simulations, namely:

(a) Fixed pressure structural optimization for low symmetry crystal unit cell.

(b) Calculation of elastic constants from the strain fluctuations.

(c) Simulation of pressure and/or temperature induced structural phase transitions.

Concerning point (a), a simple example of optimization of the crystal structure has been presented in the previous section. The possibility of obtaining the equilibrium structure by performing a single steepest descent schedule, is very appealing, particularly if compared to the more cumbersome procedure of linear interpolation of the stress components proposed by Nielsen and Martin[13]. The only limitation of the method formulated above, is due to the constant plane–wave number condition (see previous section), which restrict its applicability to systems not requiring a very large cut–off.

Concerning point (b), Parrinello and Rahman[23] first showed that elastic strain fluctuation in the (H,p,N) ensemble are a direct measure of the elastic constants in a general anisotropic medium, *i.e.*:

$$\langle \delta\epsilon_{ij}\delta\epsilon_{kl}\rangle_{HpN} = \frac{k_B\langle T\rangle}{\Omega}(C^S)^{-1}_{ijkl}, \tag{26}$$

where C^S is the matrix of the adiabatic elastic constants. If applied within our scheme, Eq. 26 allows the *ab–initio* evaluation of elastic constants by averaging over the trajectories of the isoenthalpic simulation, generated by Eqs. 18, 19. Still, due to the constant plane–wave constraint, the method is restricted to systems requiring not too large cut–off. An interestig aspect of Eq. 26 is that it can be applied also to non–crystalline systems, *e.g.* to the determination of *ab–initio* elastic constants in amorphus silicon.

Concluding with point (c), the *ab–initio* simulation of structural phase transition at constant pressure suffers the same limitations of its classical

counterpart. Since the PR trajectories sample the (H,p,N) statistical ensamble, one could in principle simulate a first or second order structural phase transition, from, say, a phase A to a phase B. In a second order phase transition the critical pressure should be related to phonon mode softening or to the vanishing of some elastic moduli. In this case one could expect a simultaneus transition of a large part of the sample from phase A to B. In the case of a first order phase transition, the two phases coexist at the transition pressure. An energy barrier separate them and temperature must be added to the ions, in order to overcome the barrier. However if one is not interested in the determination of the transition pressure, but just in the determination of the structure of the stable high pressure phase, the transition can be fastened by increasing the pressure up to an instability point.

A further complication in the *ab–initio* simulation is connected to the Fermi surface sampling. In many cases structural phase transitions are accompained by strong rearrangement of the Fermi surface – such as the insulator–metal pressure induced transition in crystalline silicon. To correctly simulate this process, the restriction of having fixed occupation numbers, f_i in the formulation above presented, will be a very relevant shortcome. However one can hope that using only the Γ point sampling and performing electronic minimizations in proximity of a level crossing, also this kind of situations can effectively be menaged.

Apart from all this technical problems, we stress that by performing simulated annealing (on the extended Lagrangian system), the method presented in the present work is able, at least in principle, to automatically find the stable structure corresponding to a given thermodynamic condition (pT).

Appendix

We will here briefly describe the specific form of DFT–LDA total energy functional used in our version of the CP *FORTRAN* code. We will also present the explicit formulas for the various contribution of this functional to the stress tensor.

Let us start from Eq. 20. To efficiently treat the slowly decaying Coulomb forces present in the second, third and last term of this equation, it is convenient to regard the ionic core charges as smeared Gaussian distributions of width R_c, centered at the ionic sites, instead of treating them as point charges. With this choice we can rewrite Eq 20 as:[11,24]

$$E = E_{ke} + E_{xc} + E_{loc}^{ps} + E_{nl}^{ps} + E_H + E_{sr} - E_{self}, \qquad (27)$$

where all terms, except E_{xc}, are written in Fourier space. E_{ke} is the electronic kinetic energy, E_{xc} the exchange–correlation energy. The electron–ion interaction energy is written as the sum of two part, the *local* (E_{loc}^{ps}) and the *non-local* (E_{nl}^{ps}) contribution. E_H is the electrostatic energy of the *total* charge distribution (electronic density ρ_e and smeared ionic charge density ρ_{ion}); E_{self} is the constant self–interaction of the ionic charges, and E_{sr} a corrective term dependig only on the ionic positions, which cancels the error introduced in considering Gaussian ionic charges insted of point charges.[11,24]

For E_{xc} it is used the LDA form, *i.e.* the exchange–correlation energy density is locally approximated by the one of the omogeneous electron gas at the same density $\rho_e(\mathbf{r})$, such as:

$$E_{xc}[\rho_e] = \int \mathrm{d}\mathbf{r} \rho_e(\mathbf{r}) \epsilon_{xc}(\rho_e(\mathbf{r})), \qquad (28)$$

where $\epsilon_{xc}(\rho_e)$ is the exchange–correlation energy density of the omogeneous electron gas at density ρ_e.

Concerning the pseudopotentials, let $v_l(r)$ be the component of the non–local pseudopotential acting on the state with l angular momentum, $v_{l_m}(r)$ the one corresponding to the state with highest angular momentum treated in the non–local form,[15] and $\delta v_l = v_l - v_{l_m}$. We write the non–local part of the pseudopotential in the separable form of Kleinman–Bylander.[22] It is also

25

convenient to define:

$$\alpha_{l,m} = \langle \varphi_{l,m} | \delta v_l | \varphi_{l,m} \rangle^{-1}, \tag{29}$$

$$F_{I,i}^{l,m} = \sum_{\mathbf{q}} c_i(\mathbf{q}) e^{i\mathbf{G}\cdot\mathbf{R}_I} \langle \delta v_l \varphi_{l,m} Y_{l,m} | \mathbf{G} \rangle, \tag{30}$$

where $Y_{l,m}$ is the spherical harmonic function with indices l, m, $|\varphi_{l,m}\rangle$ is the atomic radial pseudo–wavefunction[15] corresponding to v_l, and $|\mathbf{G}\rangle$ the plane-wave with wave vector $\mathbf{G}$.

With this choiche, the local part of the pseudopotentials is $v_{loc} = v_{lr} + v_{l_m}$, where, in the Fourier space:

$$v_{lr}(\mathbf{G}) = -\frac{Z_v}{\Omega}\frac{4\pi}{G^2}\left[\sum_{i=1}^{2} C_i \exp\left(-\frac{R_i^{c2}G^2}{4}\right) - \exp\left(-\frac{R_c^2 G^2}{4}\right)\right], \tag{31}$$

$$v_{l_m}(\mathbf{G}) = \frac{1}{\Omega}\sum_{i=1}^{3}(\pi R_i^2)^{3/2}\exp\left(-\frac{R_i^2 G^2}{4}\right)\left[A_i + B_i R_i^2\left(\frac{3}{2} - \frac{R_i^2 G^2}{4}\right)\right] \tag{32}$$

Here $R_i^c = 1/\sqrt{\alpha_i^c}$ and $R_i = 1/\sqrt{\alpha_i}$. α_i^c, C_i, α_i, A_i, and B_i are the fitting parameters defined by Bachelet, Hamann and Schlüter.[15] A_i, B_i and R_i in Eq. 32 correspond to the highest angular momentum l_m.

The terms of the total energy E (Eq. 27) are implemented in the CP *FORTRAN* code by the following formulas:

$$E_{ke} = \frac{1}{2}\sum_{i=1}^{M} f_i \sum_{\mathbf{q}} G^2 c_i^*(\mathbf{q}) c_i(\mathbf{q}) \tag{33}$$

$$E_{xc} = \int d\mathbf{r}\, \epsilon_{xc}(\rho_e(\mathbf{r}))\rho_e(\mathbf{r}) \tag{34}$$

$$E_{loc}^{ps} = \Omega \sum_{\mathbf{q}} \rho_e^*(\mathbf{G}) S(\mathbf{G}) v_{loc}(\mathbf{G}) \tag{35}$$

$$E_{nl}^{ps} = \sum_{I=1}^{N}\sum_{i=1}^{M}\sum_{l,m} f_i \alpha_{l,m} |F_{I,i}^{l,m}|^2 \tag{36}$$

$$E_H = \frac{4\pi\Omega}{2}\sum_{\mathbf{q}\neq 0} \rho_T^*(\mathbf{G})\frac{1}{G^2}\rho_T(\mathbf{G}) \tag{37}$$

$$E_{sr} = \frac{1}{2}\sum_{I=1}^{N}\sum_{J\neq I}^{N}\frac{Z_v^2}{|\mathbf{R}_I - \mathbf{R}_J|}\, \mathrm{erfc}\left(\frac{|\mathbf{R}_I - \mathbf{R}_J|}{R_c\sqrt{2}}\right) \tag{38}$$

$$E_{self} = \frac{1}{\sqrt{2\pi}}\frac{NZ^2}{R_c}. \tag{39}$$

In the Eq. 35 $S(\mathbf{G})$ is the structure factor for the ions. Notice that in the previous formulas appear both quantities defined on the *real* and on *scaled* cell, by using the scale transformation laws for coordinates and wavefunctions in direct and Fourier space (Eqs. 2, 13, 14, 24, 25). This equations imply, for instance, that the structure factor $S(\mathbf{G})$ and $\Omega \rho_e(\mathbf{G})$ are invariant under a change of h.

Finally, we write the explicit expression for the derivative of the previous terms of E with respect to the matrix h:

$$\frac{\partial E_{ke}}{\partial \mathbf{h}_{\alpha\beta}} = -\sum_{i=1}^{M} f_i \sum_{\mathbf{q}} \mathbf{G}_\alpha \mathbf{G}_\gamma \mathbf{h}_{\gamma\beta}^{t-1} c_i^*(\mathbf{q}) c_i(\mathbf{q}) \tag{40}$$

$$\frac{\partial E_{xc}}{\partial \mathbf{h}} = \left\{ \int d\mathbf{r} \left[\epsilon_{xc}(\rho_e(\mathbf{r})) - v_{xc}(\mathbf{r}) \right] \rho_e(\mathbf{r}) \right\} \mathbf{h}^{t-1} \tag{41}$$

$$\frac{\partial E_{loc}^{ps}}{\partial \mathbf{h}_{\alpha\beta}} = -E_{loc}^{ps} \mathbf{h}_{\alpha\beta}^{t-1} + 2 \sum_{\mathbf{q}\neq 0} \rho_e^*(\mathbf{G}) S(\mathbf{G}) \left\{ \frac{\Omega v_{lr}(\mathbf{G})}{G^2} \right.$$
$$- \frac{4\pi Z_v}{G^2} \left[\sum_{i=1}^{2} \frac{C_i R_i^{c2}}{4} \exp\left(-\frac{R_i^{c2} G^2}{4} \right) - \frac{R_c^2}{4} \exp\left(-\frac{R_c^2 G^2}{4} \right) \right] \tag{42}$$
$$\left. + \sum_{i=1}^{3} (\pi R_i^2)^{3/2} \frac{R_i^2}{4} \exp\left(-\frac{R_i^2 G^2}{4} \right) \left[A_i + B_i R_i^2 \left(\frac{5}{2} - \frac{R_i^2 G^2}{4} \right) \right] \right\} \mathbf{G}_\alpha \mathbf{G}_\gamma \mathbf{h}_{\gamma\beta}^{t-1}$$

$$\frac{\partial E_{nl}^{ps}}{\partial \mathbf{h}} = 2\mathrm{Re} \left(\sum_{I=1}^{N} \sum_{i=1}^{M} \sum_{l,m} f_i \alpha_{l,m} F_{I,i}^{l,m} \frac{\partial F_{I,i}^{l,m*}}{\partial \mathbf{h}} \right) \tag{43}$$

$$\frac{\partial E_H}{\partial \mathbf{h}_{\alpha\beta}} = \left[-E_H \delta_{\alpha\gamma} + 4\pi\Omega \sum_{\mathbf{q}\neq 0} \frac{\rho_t^*(\mathbf{G})}{G^2} \left(\frac{\rho_t(\mathbf{G})}{G^2} + \frac{1}{2} \rho_{ion}(\mathbf{G}) R_c^2 \right) \mathbf{G}_\alpha \mathbf{G}_\gamma \right] \mathbf{h}_{\gamma\beta}^{t-1} \tag{44}$$

$$\frac{\partial E_{sr}}{\partial \mathbf{h}_{\alpha\beta}} = -\frac{1}{2} \sum_{I} \sum_{J\neq I} \left\{ \frac{Z_v^2}{|\mathbf{R}_I - \mathbf{R}_J|^3} \mathrm{erfc}\left(\frac{|\mathbf{R}_I - \mathbf{R}_J|}{R_c\sqrt{2}} \right) \right.$$
$$\left. + \frac{\sqrt{2}}{R_c\sqrt{\pi}} \frac{Z_v^2}{|\mathbf{R}_I - \mathbf{R}_J|^2} \exp\left(-\frac{|\mathbf{R}_I - \mathbf{R}_J|^2}{R_c\sqrt{2}} \right) \right\} (\mathbf{R}_I^\alpha - \mathbf{R}_J^\alpha)(\mathbf{R}_I^\gamma - \mathbf{R}_J^\gamma) \mathbf{h}_{\gamma\beta}^{t-1} \tag{45}$$

$$\frac{\partial E_{self}}{\partial \mathbf{h}} = 0 \,. \tag{46}$$

In Eq. 43 we do not write the explicit expression for $\partial F_{I,i}^{l,m*}/\partial \mathbf{h}$, because we have to distinguish the case of $l = 0$ (and $m = 0$) from the case of $l = 1$ (and

27

$m = 1, 2, 3$). For these derivatives we get:

$$\frac{\partial F_{I,i}^{00*}}{\partial \mathbf{h}_{\alpha\beta}} = -\frac{1}{2} F_{I,i}^{00*} \mathbf{h}_{\alpha\beta}^{t-1} + \sqrt{\frac{4\pi}{\Omega}} \sum_{\mathbf{q}} c_i^*(\mathbf{q}) e^{-i\mathbf{G}\cdot\mathbf{R}_I}$$

$$\cdot \int_0^\infty x^2 \varphi_{00}(x) \delta v_0(x) \left[j_0(Gx) - \cos(Gx) \right] dx \, \frac{\mathbf{G}_\alpha \mathbf{G}_\gamma}{G^2} \mathbf{h}_{\gamma\beta}^{t-1}, \quad (47)$$

$$\frac{\partial F_{I,i}^{1\gamma*}}{\partial \mathbf{h}_{\alpha\beta}} = -\frac{1}{2} F_{I,i}^{1\gamma*} \mathbf{h}_{\alpha\beta}^{t-1} - i\sqrt{\frac{12\pi}{\Omega}} \sum_{\mathbf{q}} c_i^*(\mathbf{q}) e^{-i\mathbf{G}\cdot\mathbf{R}_I}$$

$$\cdot \left\{ \frac{\mathbf{G}_\alpha \mathbf{G}_\gamma \mathbf{G}_\eta}{G^3} \mathbf{h}_{\eta\beta}^{t-1} \int_0^\infty x^2 \varphi_{1\gamma}(x) \delta v_1(x) \left[3j_1(Gx) - \sin(Gx) \right] dx \right.$$

$$- \frac{\mathbf{G}_\alpha}{G} \mathbf{h}_{\gamma\beta}^{t-1} \int_0^\infty x^2 \varphi_{1\gamma}(x) \delta v_1(x) j_1(Gx) dx, \quad (48)$$

where j_0 and j_1 are the Bessel functions with indices 0 and 1.

References

[1] M. Parrinello and A. Rahman, Phys. Rew. Lett. **45**, 1196 (1980).

[2] H.C. Andersen, J. Chem. Phys. **72**, 2384 (1980).

[3] see for example: L. Landau and E.M. Lifshitz, "Theory of Elasticity", (Pergamon Press, Oxford, 1959).

[4] M. Parrinello, (NATO)

[5] J.R. Ray and A. Rahman, J. Chem. Phys. **80**, 4423 (1984).

[6] R. Car and M. Parrinello, Phys. Rew. Lett. **55**, 2471 (1985).

[7] R. Car and M. Parrinello, in *Simple Molecular Systems at Very High Density* (Plenum Publishing Corp., 1989) p. 455.

[8] P. C. Hohenberg and W. Kohn, Phys. Rev. **136** B864 (1964).

[9] W. Kohn and L. J. Sham, Phys. Rev. **140**, A1133 (1965).

[10] W. Kohn and P. Vashishta, in *Theory of the Inhomogeneous Electron Gas*, ed. S. Lundqvist and N. H. March, Plenum Publishing Corp., New York (1983).

[11] G. Galli and M. Parrinello (NATO, 1991).

[12] O.H. Nielsen and R.M. Martin, Phys. Rew. Lett. **50**, 697 (1983).

[13] O.H. Nielsen and R.M. Martin, Phys. Rew. B **32**, 3780 (1985).

[14] D. R. Hamann, M. Schlüter e C. Chiang, Phys. Rev. Lett. **43**, 1494 (1979).

[15] G. B. Bachelet, D. R. Hamann e M. Schlüter, Phys. Rev. B **26**, 4199 (1982).

[16] D. M. Ceperley e B. K. Alder, Phys. Rev. Lett. **45**, 566 (1980).

[17] J. C. Perdew e A. Zunger, Phys. Rev. B **23**, 5048 (1981).

[18] about the convenience of the choice of plane–waves as basis set we refer the reader to literature, for example Ref. [11] and references therein.

[19] P. Gomes Dacosta, O.H. Nielsen and K. Kunc, J. Phys. C **19**, 3163 (1986).

[20] M.T. Yin and M.L. Cohen, Phys. Rev. B **26**, 5668 (1982).

[21] G.P. Francis and M.C. Payne, J. Phys.: Condens.Matter **2**, 4395 (1990).

[22] L. Kleinman e D. M. Bylander, Phys. Rev. Lett. **48**, 1425 (1982).

[23] M. Parrinello and A. Rahman, J. Chem. Phys. **76**, 2662 (1982).

[24] P. Focher and S. Iarlori (IBM-ECSEC Internal Report, Rome 1991).